A Fast and Rapidly Convergent Iterative Physical Optics Algorithm for Computing the RCS of Open-Ended Cavities

Robert J. Burkholder
The Ohio State University Department of Electrical Engineering
ElectroScience Laboratory, 1320 Kinnear Road, Columbus, OH 43212
E-mail: burkhold@ee.eng.ohio-state.edu

Abstract—**Two major enhancements to the iterative physical optics (IPO) method are described for analyzing the EM scattering from open-ended cavities. First, a Jacobi Minimal Residual (JMRES) iterative algorithm is developed which preserves the physically appealing nature of IPO while establishing robust convergence criteria based on minimizing the residual error. It is shown that the JMRES algorithm usually converges much faster than conjugate gradient based methods for cavities. Second, a form of the fast far field approximation (FaFFA) is implemented to accelerate the computation of the integral operator in IPO. The FaFFA decreases the CPU time by a factor of about $\frac{1}{5}N^{\frac{1}{3}}$, where N is the number of surface integration sample points. These improvements allow much larger and more realistically complex cavities to be analyzed with fast IPO.**

Keywords—**Electromagnetic scattering, Radar cross sections, Cavities, Iterative methods, Physical optics.**

I. Introduction

The iterative physical optics (IPO) method was developed to analyze the electromagnetic (EM) scattering from arbitrarily shaped open-ended cavities which are large with respect to wavelength [1]. As its name implies, the principles of physical optics (PO) are applied iteratively to evaluate the equivalent surface currents on the inner walls of the cavity. The iterative re-radiation of the wall currents accounts for the multiple reflections inside the cavity. IPO was developed to handle arbitrarily shaped cavities for which the waveguide modal method [2] is not applicable, because waveguide modes can only be found in closed form for a relatively small set of canonical geometries. IPO was also developed to obtain better accuracy than ray-based methods, such as the shooting and bouncing ray (SBR) method [2], [3], [4], and the generalized ray expansion (GRE) method [4], [5]. It has been combined with the termination reciprocity integral [6] to handle cavities with very complex terminations, such as a jet engine cavity [7].

This paper addresses two major problems associated with IPO: convergence and computational efficiency. First, no solid convergence criterion has been established for halting the iterations. It has been based on *a priori* knowledge of the cavity geometry by guessing the maximum number of internal reflections which will be significant as a function of aspect angle [1]. Furthermore, as a classical (stationary) iterative method [8], the solution may diverge if too many iterations are performed because the iteration matrix may have a spectral radius greater than unity. Second, in terms of efficiency the IPO method is limited by an $\mathcal{O}(N^2)$ operational count per iteration, where N is the total number of integration sample points. The iterative equation for IPO is very similar to the magnetic field integral equation (MFIE) [9]; however, the numerical sampling density of the surface currents corresponds to PO, which is far less than rigorous integral equation methods (i.e., 4 to 9 samples per square wavelength, instead of 64 to 100). The operational count per iteration of IPO is $\mathcal{O}(N^2)$ because each current element radiates to (nearly) all other current elements at each iteration. Even though IPO uses a small number of sample points per wavelength, the $\mathcal{O}(N^2)$ computational cost limits the size of the cavity geometry.

It is known that conjugate gradient based iterative solutions to cavity problems are slowly convergent [10]. The convergence issue is addressed here by introducing a new iterative algorithm which may be applied to IPO. The algorithm is a form of Jacobi iteration [8], which is optimized here using two degrees of freedom to minimize the residual error at each step. The new algorithm is referred to as the *Jacobi Minimal Residual* (JMRES) method, and is described in Section III. It preserves the physical interpretation of IPO, i.e., each iteration accounts for another internal reflection, while guaranteeing a non-diverging solution. The algorithm is shown to converge after a relatively small number of iterations, starting with the first order PO currents as the initial guess, and the number of iterations tends to depend on the geometry and incidence angle rather than the number of unknowns. The JMRES algorithm is a reduced form of the generalized minimal residual (GMRES) method [11] which is also applied here to IPO. The GMRES algorithm is shown to be much more rapidly convergent than the conjugate and bi-conjugate

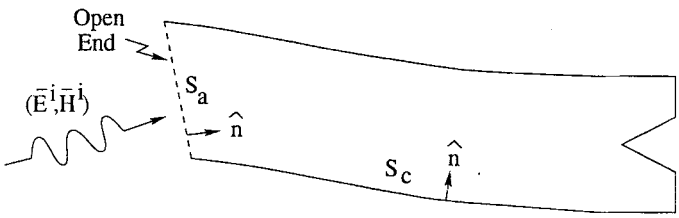

Fig. 1. Open-ended cavity illuminated by an incident field.

gradient methods [12], [13] when applied to cavities.

The efficiency of IPO is substantially improved by implementing a form of the *Fast Far Field Approximation* (FaFFA) [14]. The FaFFA is similar to the fast multipole method (FMM) [15], but is much easier to implement. The FaFFA accelerates the $\mathcal{O}(N^2)$ operation associated with the re-radiation of the surface currents at each iteration, reducing it by a factor of about $\frac{1}{5}N^{\frac{1}{3}}$ (for a sampling density of 9 points per square wavelength). The FaFFA as applied to IPO is referred to here as *Fast IPO* (FIPO), and is described in Section IV.

Numerical results demonstrating the convergence properties, accuracy, and efficiency of the algorithms proposed here are presented in Section V. Conclusions are discussed in Section VI. The original IPO algorithm is first briefly described in the next section.

II. The IPO Method

Figure 1 shows the geometry of an arbitrarily shaped open-ended cavity with the aperture illuminated by an incident EM field. S_a is the aperture surface and S_c is the surface of the inner cavity walls. The cavity walls are assumed here to be perfect electrical conductors (PEC), but the formulation may be easily extended to impenetrable material walls using a surface impedance boundary condition [16]. An $e^{j\omega t}$ harmonic time convention is assumed and suppressed in the following. λ and k are the wavelength and wavenumber, respectively, of the incident EM field in the ambient media which is assumed to be free space.

The cavity geometry and aperture are replaced with equivalent surface currents which radiate in free space. The approximate magnetic field integral equation (MFIE) for finding the electric surface current $\bar{J}$ at points $\bar{r}_c$ on the cavity walls is given by [1]:

$$\bar{J}(\bar{r}_c) = 2\hat{n}\times\bar{H}^i_c(\bar{r}_c) + 2\hat{n}\times\int\!\!\!\!\!\!-_{S_c}\bar{J}(\bar{r}')\times\hat{R}'\,\frac{e^{-jkR'}}{4\pi R'}\left(jk+\frac{1}{R'}\right)dS' \quad (1)$$

where $\bar{R}' = \bar{r}_c - \bar{r}'$, $R' = |\bar{R}'|$, $\hat{R}' = \bar{R}'/R'$, $\bar{r}'$ is an integration point on the surface S_c, and $\int\!\!\!\!\!\!-$ denotes the principal value integral. $\bar{H}^i_c(\bar{r}_c)$ is the incident magnetic field on the cavity walls radiated by the Kirchhoff aperture currents defined by

$$\begin{aligned}\bar{J}^i_a(\bar{r}_a) &= \hat{n}\times\bar{H}^i(\bar{r}_a)\\ \bar{M}^i_a(\bar{r}_a) &= \bar{E}^i(\bar{r}_a)\times\hat{n}\end{aligned} \quad (2)$$

where $\bar{r}_a$ is a point on the aperture surface S_a. Eq. (2) is approximate because the Kirchhoff approximation has been used for the aperture currents [2]. Otherwise, to find the aperture currents rigorously it is necessary to write a second integral equation for the external region which is coupled to the cavity via the aperture currents. The resulting equations are solved simultaneously using a direct solution as in [10], [17], or an iterative solution as in [18]. The Kirchhoff approximation used here has been shown to be very accurate for electrically large apertures as long as the incident field is not close to grazing the aperture [2].

The rules of IPO state that the integral in (2) is evaluated only over the portion of S_c where $\bar{n}\cdot\bar{R}' < 0$. In other words, source points only radiate to points on S_c which are facing them, ignoring any intervening geometry. The same rule is followed in evaluating the incident magnetic fields $\bar{H}(\bar{J}^i_a)$ and $\bar{H}(\bar{M}^i_a)$ on S_c. The original IPO paper [1] used more rigorous shadowing rules, but the new $\bar{n}\cdot\bar{R}' < 0$ rule has been found to give better convergence and is very easy to implement.

The integral equation of (2) is discretized using point sampling with a sampling density of 4 to 9 points/λ^2. The surfaces are assumed to be locally flat at the sample points, and two orthogonal current directions are defined at each point. In the original IPO method the following iterative equation is used to find $\bar{J}$ for the ℓ^{th} iteration:

$$\bar{J}^{(\ell)}(\bar{r}_c) = 2\hat{n}\times\bar{H}^i_c(\bar{r}_c) + 2\hat{n}\times\int\!\!\!\!\!\!-_{S_c}\bar{J}^{(\ell-1)}(\bar{r}')\times\hat{R}'\,\frac{e^{-jkR'}}{4\pi R'}\left(jk+\frac{1}{R'}\right)dS' \quad (3)$$

starting with an initial guess of

$$\bar{J}^{(0)}(\bar{r}_c) = 2n\times\bar{H}^i_c(\bar{r}_c) \quad (4)$$

which is the first order PO current on the cavity walls. Each iteration adds another internal reflection of the cavity fields. The iteration halts after a pre-specified number of steps based on the number of expected internal reflections, or when the relative change in the currents becomes small enough to neglect subsequent iterations. However, the number of internal reflections is generally not known *a priori*, and the algorithm is likely to diverge after too many iterations for reasons discussed in the next section.

Once (2) is solved for $\bar{J}$ using IPO, the Kirchhoff approximation is again used to find the scattered equivalent currents in the aperture, and the cavity scattered fields in the external region may then be found via aperture integration.

III. The JMRES Algorithm

Eq. (2) can be written in operator notation as

$$\bar{\bar{Z}}\bar{J} = \bar{J}^i \tag{5}$$

where

$$\bar{\bar{Z}}\bar{J} = \bar{J} - 2\hat{n} \times \int_{S_c} \bar{J} \times \hat{R}' \frac{e^{-jkR'}}{4\pi R'} \left(jk + \frac{1}{R'}\right) dS' \tag{6}$$

$$\bar{J}^i = 2\hat{n} \times \bar{H}^i_c. \tag{7}$$

The residual error vector at the ℓ^{th} iteration step is defined as

$$\bar{\mathcal{R}}^{(\ell)} = \bar{J}^i - \bar{\bar{Z}}\bar{J}^{(\ell)} \tag{8}$$

It is clear that the error vector goes to zero if $\bar{J}^{(\ell)}$ satisfies (2), or equivalently, if $\bar{J}^{(\ell)} = \bar{J}^{(\ell-1)}$ in (4). The residual error norm, usually referred to as simply the *Residual Error*, is given by

$$\text{Residual Error} = \sqrt{\frac{<\bar{\mathcal{R}}^{(\ell)}, \bar{\mathcal{R}}^{(\ell)}>}{<\bar{J}^i, \bar{J}^i>}} \tag{9}$$

where the inner product of two vector functions existing over the surface S_c is defined by

$$<\bar{A}, \bar{B}> = \int_{S_c} \bar{A}^*(\bar{r}') \cdot \bar{B}(\bar{r}')\, dS'. \tag{10}$$

The residual error is a measure of how well the solution satisfies the original discretized integral equation.

The basic IPO equation (4) may be re-written in terms of the residual error vector as

$$\bar{J}^{(\ell)} = \bar{J}^{(\ell-1)} + \bar{\mathcal{R}}^{(\ell-1)}. \tag{11}$$

This equation has the form of a stationary Jacobi iteration, and it is not guaranteed to converge to a stable solution unless the spectral radius of the iteration matrix is less than unity [8]. If a relaxation parameter α is introduced the equation becomes

$$\bar{J}^{(\ell)} = \bar{J}^{(\ell-1)} + \alpha\bar{\mathcal{R}}^{(\ell-1)}. \tag{12}$$

This equation *may* converge if α is chosen based on *a priori* knowledge of the eigenvalue distribution of the system matrix. Alternatively, a new α may be found at each iteration which minimizes the ℓ^{th} residual error. Taking this idea one step further, the following iterative form is proposed:

$$\bar{J}^{(\ell)} = \alpha_1 \bar{J}^{(\ell-1)} + \alpha_2 \bar{\mathcal{R}}^{(\ell-1)}, \tag{13}$$

where α_1 and α_2 are chosen to minimize the norm of $\bar{\mathcal{R}}^{(\ell)}$ as follows.

$$\bar{\mathcal{R}}^{(\ell)} = \bar{J}^i - \alpha_1 \bar{\bar{Z}}\bar{J}^{(\ell-1)} - \alpha_2 \bar{\bar{Z}}\bar{\mathcal{R}}^{(\ell-1)} \tag{14}$$

$\bar{J}^{(0)} = \bar{J}^i$
$\bar{\mathcal{R}}^{(0)} = \bar{J}^i - \bar{\bar{Z}}[\bar{J}^{(0)}]$
For $\ell = 1, 2, ...$
  $\bar{q}_1 = \bar{\bar{Z}}\bar{J}^{(\ell-1)} = \bar{J}^i - \bar{\mathcal{R}}^{(\ell-1)}$
  $\bar{q}_2 = \bar{\bar{Z}}\bar{\mathcal{R}}^{(\ell-1)}$
  $H_{11} =< \bar{q}_1, \bar{q}_1 >$
  $H_{12} =< \bar{q}_1, \bar{q}_2 >$
  $H_{21} = H^*_{12}$
  $H_{22} =< \bar{q}_2, \bar{q}_2 >$
  $v_1 =< \bar{q}_1, \bar{J}^i >$
  $v_2 =< \bar{q}_2, \bar{J}^i >$
  Solve $[H][\alpha] = [v]$
  $\bar{J}^{(\ell)} = \alpha_1 \bar{J}^{(\ell-1)} + \alpha_2 \bar{\mathcal{R}}^{(\ell-1)}$
  $\bar{\mathcal{R}}^{(\ell)} = \bar{J}^i - \alpha_1 \bar{q}_1 - \alpha_2 \bar{q}_2$
  Check residual error.
End

Fig. 2. The JMRES algorithm.

$$<\bar{\mathcal{R}}^{(\ell)}, \bar{\mathcal{R}}^{(\ell)}> = <\bar{J}^i, \bar{J}^i> + |\alpha_1|^2 <\bar{\bar{Z}}\bar{J}^{(\ell-1)}, \bar{\bar{Z}}\bar{J}^{(\ell-1)}> + |\alpha_2|^2 <\bar{\bar{Z}}\bar{\mathcal{R}}^{(\ell-1)}, \bar{\bar{Z}}\bar{\mathcal{R}}^{(\ell-1)}> - 2\text{Re}\left[\alpha_1^* <\bar{\bar{Z}}\bar{J}^{(\ell-1)}, \bar{J}^i> + \alpha_2^* <\bar{\bar{Z}}\bar{\mathcal{R}}^{(\ell-1)}, \bar{J}^i>\right] \tag{15}$$

where the property $<\bar{A}, \bar{B}>=<\bar{B}, \bar{A}>^*$ has been employed. Taking partial derivatives of (15) with respect to the real and imaginary parts of α_1 and α_2 and setting the resulting equations equal to zero yields the following 2×2 system of equations:

$$\begin{bmatrix} <\bar{\bar{Z}}\bar{J}^{(\ell-1)}, \bar{\bar{Z}}\bar{J}^{(\ell-1)}> & <\bar{\bar{Z}}\bar{J}^{(\ell-1)}, \bar{\bar{Z}}\bar{\mathcal{R}}^{(\ell-1)}> \\ <\bar{\bar{Z}}\bar{\mathcal{R}}^{(\ell-1)}, \bar{\bar{Z}}\bar{J}^{(\ell-1)}> & <\bar{\bar{Z}}\bar{\mathcal{R}}^{(\ell-1)}, \bar{\bar{Z}}\bar{\mathcal{R}}^{(\ell-1)}> \end{bmatrix} \begin{bmatrix} \alpha_1 \\ \alpha_2 \end{bmatrix} = \begin{bmatrix} <\bar{\bar{Z}}\bar{J}^{(\ell-1)}, \bar{J}^i> \\ <\bar{\bar{Z}}\bar{\mathcal{R}}^{(\ell-1)}, \bar{J}^i> \end{bmatrix} \tag{16}$$

This iterative approach preserves the physically insightful nature of IPO while minimizing the residual at each step. Since the solution vector at the ℓ^{th} step is a linear combination of the solution and residual error vectors of the previous step, the minimized residual error is guaranteed to be less than or equal to the residual error of the previous step. The complete JMRES algorithm is shown in Figure 2.

A close examination of the JMRES algorithm will reveal that it is mathematically equivalent to the GMRES algorithm [11] with a restart interval of 2. GMRES saves the search vectors from all previous iterations within the restart interval, and minimizes the residual error at each step. GMRES also orthogonalizes the search vectors, but the same solution space is spanned with or without orthogonalization. GMRES requires a large amount of computer memory, depending on the restart interval. As the numerical results of Section V will show, JMRES has nearly the same convergence when applied to cavity

problems as the full (not restarted) GMRES algorithm. Furthermore, JMRES is much easier to implement than GMRES and requires far less storage (only $5N$ complex variables as opposed to $3N + mN$ for GMRES, where m is the number of iterations done before restarting). It is noted, however, that GMRES is guaranteed to reduce the residual error to zero after N iterations (assuming no restarts, and machine precision permitting) because it spans the entire solution space. It also has much faster convergence than the conjugate and bi-conjugate gradient methods for cavities, as the numerical results will show.

Finally, it is noted that the computationally expensive evaluation of the operator $\overline{\overline{Z}}$ needs to be done only once per iteration in JMRES and GMRES, which is an $\mathcal{O}(N^2)$ operation. This is in contrast to conjugate gradient based methods for non-Hermitian systems which generally require two of these operations per iteration [12], [13]. Furthermore, they also usually require that the Hermitian adjoint operator $\overline{\overline{Z}}^{\mathrm{H}}$ be computed as one of these operations. However, $\overline{\overline{Z}}^{\mathrm{H}}$ is not straightforward to define for the non-reciprocal IPO operator, especially when it is accelerated using the FaFFA method of the next section.

IV. FaFFA Acceleration

The FaFFA [14] accelerates the computation of the surface current radiation integral,

$$\bar{H}(\bar{r}) = \int_{S_c} \bar{J}(\bar{r}') \times \hat{R}' \frac{e^{-jkR'}}{4\pi R'} \left(jk + \frac{1}{R'} \right) dS' \quad (17)$$

which is the most time-consuming operation in evaluating $\overline{\overline{Z}}\bar{J}$. The integral is computed at every sample point $\bar{r}_c$, which requires $\mathcal{O}(N^2)$ operations if done with straightforward numerical integration.

The FaFFA is very similar to the FMM [15] in that the unknown current elements are spatially grouped as shown in Figure 3, and the radiation integral is evaluated one pair of groups at a time. For groups which are separated by less than the far field distance of $2D^2/\lambda$, the integral is computed using direct numerical integration. If there are approximately M elements in each group, then the numerical integration for one group radiating to another requires M^2 operations. For groups separated by more than the far field distance, the following far field approximation is used for (17):

$$\bar{H}_{pq}(\bar{r}) \approx \bar{H}_{pq}(\bar{r}_q)\, e^{-jk(\bar{r}-\bar{r}_q)\cdot\hat{R}_{pq}} \quad (18)$$

where $\bar{H}_{pq}$ denotes the magnetic field radiated from source group p to far field group q, $\bar{r}_p$ and $\bar{r}_q$ are the centers of groups p and q, respectively, and $\bar{R}_{pq} = \bar{r}_q - \bar{r}_p$ as shown in Figure 3. $\bar{H}_{pq}(\bar{r}_q)$ is found first by integrating over the elements of group p. Then, (18) is used to find $\bar{H}_{pq}(\bar{r})$ for all the test points within group q. The number of operations required for evaluating (17) for this pair of groups is then reduced to $2M$ from M^2.

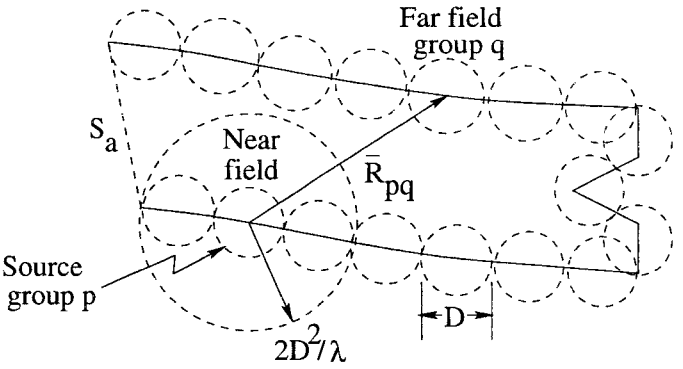

Fig. 3. Spatial grouping of surface elements for the FaFFA formulation.

Considering the savings in computing the far field group interactions compared with nearby groups, we should choose the groups to be as large as possible. However, larger groups means the far field separation distance between groups is larger, so fewer pairs of groups will be eligible for (18). A tradeoff can be reached by minimizing the total operational count as a function of M.

For a 3D cavity geometry the number of near field receiving groups within radius $2D^2/\lambda$ of a given source group is approximately

$$N_{nf} = \frac{16\pi}{N_s} M \quad (19)$$

where N_s is the number of sample points per square wavelength. Since there are N/M groups, the operational count associated with evaluating all the near field interactions is

$$C_{nf} = N_{nf} M^2 (N/M) = \frac{16\pi}{N_s} M^2 N. \quad (20)$$

Likewise, using (18) the operational count associated with evaluating all the far field interactions is

$$\begin{aligned} C_{ff} &= 2M\,(N/M - N_{nf})\,(N/M) \\ &= 2N^2/M - \frac{32\pi}{N_s} MN, \end{aligned} \quad (21)$$

and the total count is then

$$\begin{aligned} C &= C_{nf} + C_{ff} \\ &= \frac{16\pi}{N_s} M(M-2)N + 2N^2/M. \end{aligned} \quad (22)$$

Minimizing with respect to M (and assuming $M \gg 2$) yields

$$M = \left(\frac{NN_s}{16\pi} \right)^{\frac{1}{3}} \quad (23)$$

and the minimal operational count is

$$C_{min} = 3\left(\frac{16\pi}{N_s}\right)^{\frac{1}{3}} N^{\frac{5}{3}}. \quad (24)$$

For large N this is substantially lower than the N^2 operations required for direct numerical integration. It is noted that the operational count of the basic FaFFA (without the use of a discrete plane wave expansion) is claimed to be $\mathcal{O}(N^{3/2})$ in [14]. This is because the authors do not take into account the variable size of the near field region in their optimization procedure. The $\mathcal{O}(N^{3/2})$ count may be achieved if a constant number of near field groups is assumed, although it may not be optimal or it may be invalid as the group size increases.

V. Numerical Results

Figure 4 shows the RCS patterns as a function of azimuth angle for an open-ended circular cylinder with a flat termination. The waveguide modal solution has been shown to be very accurate for this type of canonical geometry, so it is used as a reference. The Direct IPO results were obtained by halting the iterations when a residual error of less than 0.1 was reached. The Fast IPO iterations were halted when a residual error of less than 0.1 and 0.05 were reached for the two curves, respectively. The three IPO curves agree very well with each other, and with the modal solution, out to about 60°. Beyond 60° the errors introduced by the approximations used in IPO and FaFFA accumulate to a noticeable degree after many iterations (see Table I below). Furthermore, the Kirchhoff approximation used for the aperture currents begins to break down, and the higher-order diffraction effects across the aperture begin to excite modes near cut-off. Since the waveguide modal results also use the Kirchhoff approximation at the aperture, these higher-order effects are not included. So, none of the results may be considered reliable beyond 60°. However, the scattering from the external geometry generally tends to become dominant over the cavity scattering at wide angles. It is noted that the FIPO method may be extended to a rigorous coupled integral equation formulation which includes the external region, as in [18].

As Figure 4 shows, the FaFFA introduces a small error in the evaluation of the integral operator $\overline{\overline{Z}}$ compared with direct IPO integration, but is only noticeable for very wide angles of incidence. The cavity walls are discretized with 9 facets/λ^2 for a total of $N = 6,600$ facets. The IPO results took a total of 31 hours and 14 minutes on an SGI Indy Workstation with a 150 MHz R4400 processor and 96 MB RAM. The patterns are computed at 2° increments in azimuth. The FIPO results took 11 hours and 6 minutes on the same machine, which is a factor of 2.8 speed-up. Equation (24) predicts a speed-up factor of 3.5 compared with the N^2 operations needed per

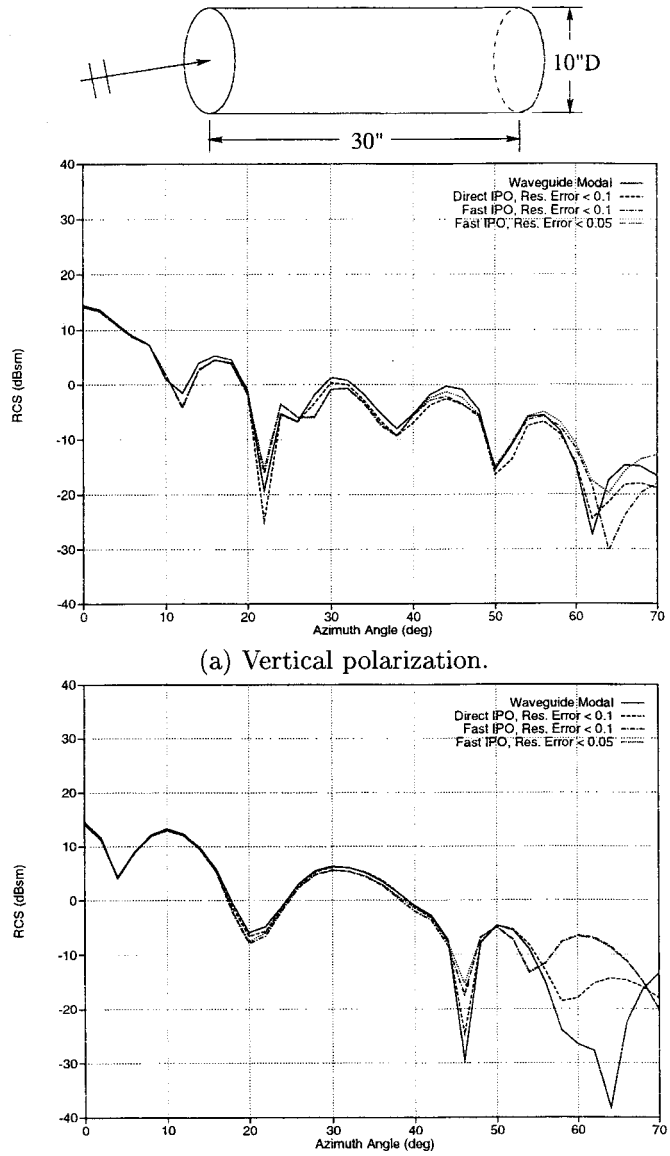

Fig. 4. RCS patterns of a circular waveguide cavity at 10 GHz. The JMRES algorithm is used for all the IPO results with 9 facets/λ^2 sampling density.

iteration without FaFFA. The actual speed-up is lower than predicted because (24) assumes an optimal grouping of elements in FaFFA, such that all the groups have the same number of elements and are about the same size. In practice, this is very difficult to achieve for realistic geometries. Furthermore, IPO with FaFFA required slightly more iterations for convergence than IPO without FaFFA because of the small amount of error introduced by the far field approximation. It is noted that the approximation may be improved by simply defining a larger far field distance, but at the cost of reduced efficiency.

Figure 5 plots the residual error curves for the same geometry for a wide aspect angle of 60°. The residual error

curves for the conjugate gradient method (CGM) and the bi-conjugate gradient stabilized method (BiCGStab) [19] are also shown in Figure 5 for comparison. The FaFFA is not used here with the CGM because of the difficulties in evaluating the Hermitian adjoint operator with FaFFA. Furthermore, since the CGM requires the $\overline{\overline{Z}}$ and $\overline{\overline{Z}}^{H}$ integral operators to each be evaluated for every iteration, the number of iterations in Figure 5 is actually the number of times the integral operator is computed for the CGM results. The BiCGStab results use FaFFA, but the integral operator is computed twice per iteration also, so the number of integral operator computations is plotted. This provides a more direct comparison in terms of the most computationally expensive step in the algorithms. The convergence of CGM is much slower than GMRES, and BiCGStab is better than CGM but more erratic and not as fast as GMRES. JMRES, which is equivalent to GMRES with a restart interval of 2, has nearly the same convergence as GMRES down to a residual error level of 0.05. Beyond 0.05 the algorithms start flattening out, most likely due to the approximations associated with IPO and FaFFA. However, it has been found that a residual error level of 0.1 gives sufficiently accurate RCS results for most cavity scattering applications.

Table I shows the number of iterations as a function of the azimuth angle for the JMRES/FIPO results of Figure 4 with a residual error threshold of 0.1. As expected from the physical interpretation of IPO, the number of iterations is closely related to the number of dominant internal reflections for this simple geometry. For more complex geometries the number of internal reflections may not be easy to guess *a priori*. That is why the new JMRES algorithm is especially valuable—the residual error can be easily monitored to indicate when the solution has sufficiently converged, and the number of iterations provides the maximum number of significant internal reflections.

TABLE I
NUMBER OF ITERATIONS FOR CYLINDRICAL CAVITY (RESIDUAL ERROR < 0.1).

	V-Pol.	H-Pol.
0°	4	4
10°	5	4
20°	9	7
30°	12	10
40°	18	16
50°	23	22
60°	28	34
70°	33	59

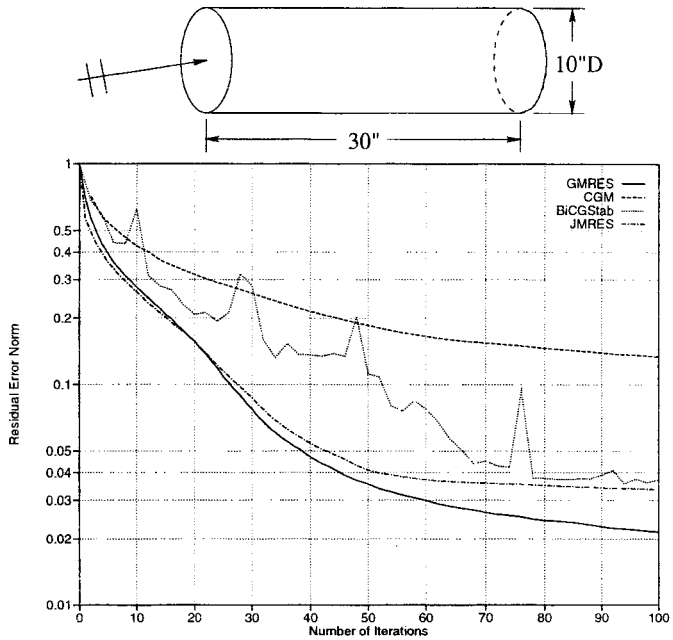

(a) Vertical polarization.

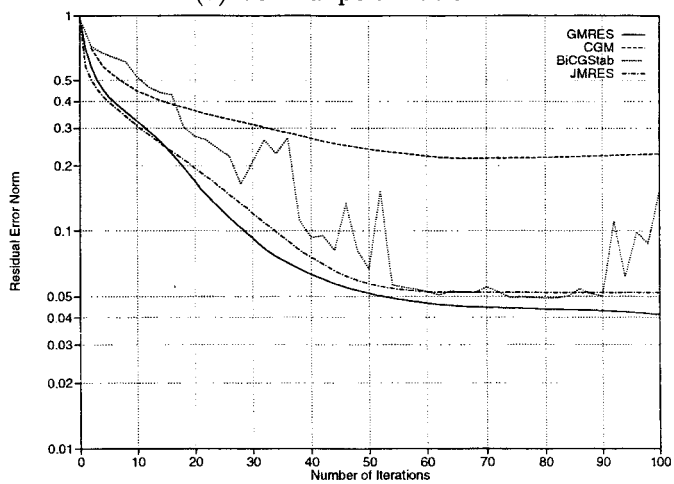

(b) Horizontal polarization.

Fig. 5. Error curves of a circular waveguide cavity at 10 GHz, illuminated 60° off-axis. 9 facets/λ^2 are used in the IPO algorithm. GMRES, BiCGStab and JMRES use FIPO.

Figure 6 shows the RCS patterns of a realistically complex cavity computed using the FIPO/JMRES algorithm. The geometry is represented by a facet model generated by ACAD [20], and is compatible with the XPATCH code [21]. The exact dimensions of the cavity are too cumbersome to include here, but the ACAD file is available from the sponsors listed in the Acknowledgements (U.S. only). 8,122 facets are used with an average sampling density of 14.3 facets/λ^2. The patterns took a total of 33 hours and 19 minutes to compute on the SGI Indy (computed at 2° increments in azimuth angle). The minimum and maximum number of iterations for convergence are 43 and 79, respectively. As one would expect, this complex cavity requires more iterations than the simple cylindrical cav-

ity. As with the cylinder RCS results, only the scattering from the cavity interior is included in the calculation, with no external scattering.

VI. Conclusions

Two major enhancements to the basic IPO method for cavity scattering problems have been demonstrated: (1) a robust convergence criteria based on the residual error of the newly introduced JMRES iterative algorithm, and (2) acceleration of the numerical integration using the FaFFA. Convergence is reached in a relatively small number of iterations using the JMRES algorithm, and the physical insight of IPO is preserved. A residual error threshold of 0.1 is seen to be sufficient for cavity RCS problems. The GMRES algorithm is also found to be very useful for cavities, having much faster convergence than gradient methods, but the storage requirement may be excessive.

The simple version of FaFFA used here reduces the operational count per iteration by a factor of about $\frac{1}{5}N^{\frac{1}{3}}$ compared with direct numerical integration, with a small degradation in accuracy. The accuracy may be improved by using a larger far field group separation requirement, but at the cost of efficiency. The efficiency may be further substantially improved using the discrete plane wave expansion method described in [14], or the more sophisticated FMM [15] and accelerated versions of FMM such as in [22], but with considerably more implementation effort.

Acknowledgments

This work was supported by DEMACO, Inc. (now SAIC), under Prime Contract F33615-96-C-1937 from the Air Force Wright Laboratories Non-Cooperative Target ID program, Wright-Patterson AFB, Ohio.

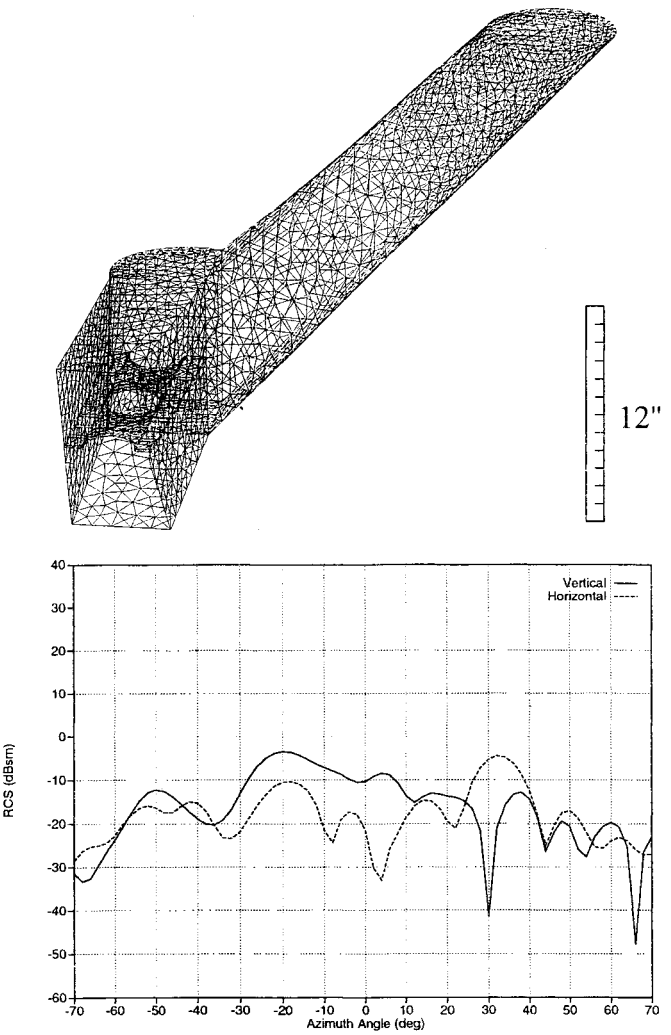

Fig. 6. Co-polarized Azimuth RCS patterns of a realistic cavity computed using the JMRES algorithm. Elevation=0°, frequency=10 GHz, residual error norm threshold=0.1. Open end of cavity is at lower left of geometry.

References

[1] F. Obelleiro, J.L. Rodriguez, and R.J. Burkholder, "An Iterative Physical Optics Approach for Analyzing the Electromagnetic Scattering by Large Open-Ended Cavities," *IEEE Trans. Antennas and Propagation*, Vol. 43, No. 4, pp. 356-361, April 1995.

[2] P.H. Pathak and R.J. Burkholder, "Modal, Ray and Beam Techniques for Analyzing the EM Scattering by Open-Ended Waveguide Cavities," *IEEE Trans. Antennas and Propagat.*, Vol. AP-37, No. 5, pp. 635-647, May 1989.

[3] H. Ling, R.C Chou, and S.W. Lee, "Shooting and Bouncing Rays: Calculating RCS of an Arbitrary Cavity," *IEEE Trans. Antennas and Propagat.*, Vol. 37, No. 2, pp. 194-205, February 1989.

[4] R.J. Burkholder, R.-C. Chou, and P.H. Pathak, "Two Ray Shooting Methods for Computing the EM Scattering by Large Open-Ended Cavities," invited paper to *Computer Physics Communications - Thematic issue on Computational Electromagnetics*, Vol. 68, Nos. 1-3, pp. 353-365, Nov. 1991.

[5] P.H. Pathak and R.J. Burkholder, "High Frequency Electromagnetic Scattering by Open-Ended Waveguide Cavities," *J. Radio Science*, Vol. 26, No. 1, pp. 211-218, Jan.-Feb. 1991.

[6] P.H. Pathak and R.J. Burkholder, "A Reciprocity Formulation for Calculating the EM Scattering by an Obstacle within an Open-Ended Waveguide Cavity," *IEEE Transactions on Microwave Theory and Techniques*, Vol. 41, No. 4, pp. 702–707, April 1993.

[7] T.-T. Chia, R.J. Burkholder, and R. Lee, "The Application of FDTD in Hybrid Methods for Cavity Scattering Analysis," *IEEE Trans. Antennas and Propagat.*, Vol. 43, No. 10, pp. 1082-1090, October 1995.

[8] G.H. Golub and C.F. Van Loan, Chapter 10 in *Matrix Computations*, Second Edition, The Johns Hopkins University Press, Baltimore, 1989.

[9] R.F. Harrington, *Field Computation by Moment Methods*, New York: Macmillan, 1968.

[10] C.-C. Lu and W.C. Chew, "A New-Resonance Decoupling Approach (NRDA) for Scattering Solution of Near-Resonant Structures," *IEEE Trans. Antennas and Propagat.*, Vol. 45, No. 12, pp. 1857-1862, December 1997.

[11] Y. Saad and M.H. Schultz, "GMRES: A generalized minimal

residual algorithm for solving non-symmetric linear systems, *SIAM J. Sci. Statist. Comput.*, Vol. 7, pp. 856-869, March 1986.

[12] T.K. Sarkar and E. Arvas, "On a Class of Finite-Step Iterative Methods (Conjugate Directions) for the Solution of an Operator Equation Arising in Electromagnetics," *IEEE Trans. Antennas and Propagat.*, Vol. 33, No. 9, pp. 1058-1066, Oct. 1985.

[13] C.F. Smith, A.F. Peterson, and R. Mittra, "The Biconjugate Gradient Method for Electromagnetic Scattering," *IEEE Trans. Antennas and Propagat.*, Vol. 38, No. 6, pp. 938-940, June 1990.

[14] C.C. Lu and W.C. Chew, "Fast Far-Field Approximation for Calculating the RCS of Large Objects," *Microwave Opt. Tech. Letters*, Vol. 8, No. 5, pp. 238-241, 1995.

[15] R. Coifman, V. Rokhlin, and S. Wandzura, "The Fast Multipole Method for the Wave Equation: A Pedestrian Prescription," *IEEE Antennas and Propagation Magazine*, Vol. 35, No. 3, pp. 7-12, 1993.

[16] K.M. Mitzner, "An Integral Equation Approach to Scattering from a Body of Finite Conductivity," *Radio Science*, Vol. 2 (New series), No. 12, pp. 1459-1470, Dec. 1967.

[17] T. Wang, R.F. Harrington, and J.R. Mautz, "Electromagnetic Scattering from and Transmission Through Arbitrary Apertures in Conducting Bodies," *IEEE Trans. Antennas and Propagat.*, Vol. 38, No. 11, pp. 1805-1814, Nov. 1990.

[18] D.D. Reuster and G.A. Thiele, "A Field Iterative Method for Computing the Scattered Electric Fields at the Apertures of Large Perfectly Conducting Cavities," *IEEE Trans. Antennas and Propagat.*, Vol. 43, No. 3, pp. 286-290, Mar. 1995.

[19] H. van der Vorst, "Bi-CGSTAB: A Fast and Smoothly Converging Variant of Bi-CG for the Solution of Non-symmetric Linear Systems," *SIAM J. Sci. Statist. Comput.*, Vol. 13, pp. 631-644, 1992.

[20] ACAD Technical Manual, Lockheed Martin Corporation, Fort Worth, Texas, April 1995.

[21] D.J. Andersh, M. Hazlett, S.W. Lee, D.D. Reeves, D.P. Sullivan, and Y. Chu, "XPATCH: A High Frequency Electromagnetic Scattering Code and Environment for Complex 3D Objects," *IEEE Antennas and Propagat. Magazine*, Vol. 6, pp. 65-69, February 1994.

[22] R.J. Burkholder and D.H. Kwon, "High-Frequency Asymptotic Acceleration of the Fast Multipole Method," *Radio Science*, Special Section on Computational Electromagnetics, Vol. 31, No. 5, pp. 1199-1206, September-October 1996.